AIMS Mathematics, 11(2): 3986–4007.
DOI: 10.3934/math.2026160
Received: 14 December 2025
Revised: 22 January 2026
Accepted: 04 February 2026
Published: 09 February 2026

https://www.aimspress.com/journal/Math

Research article

Analytically pricing European options under a two-factor Heston-Vasicek model with regime switching and stochastic interest rate

Xin-Jiang He[1,2] **and Sha Lin**[3,4,*]

[1] School of Economics, Zhejiang University of Technology, Hangzhou, China
[2] Institute for Industrial System Modernization, Zhejiang University of Technology, Hangzhou, China
[3] School of Finance, Zhejiang Gongshang University, Hangzhou, China
[4] School of Tailong Finance, Zhejiang Gongshang University, Hangzhou, China

* **Correspondence:** Email: linsha@mail.zjgsu.edu.cn.

Abstract: This article establishes a hybrid model by adding into the Heston-Vasicek model an additional regime switching factor, which combines the advantages of the stochastic interest rate, regime switching, and multi-factor stochastic volatility. It assumes a Vasicek stochastic interest rate, and uses two stochastic factors for asset volatility, one of which follows Heston stochastic volatility and another can switch according to a continuous-time Markov chain. Such a setting considers both effects of economic cycles and the correlation between the stock and interest rate, while still ensuring the existence of an analytical solution for European option pricing. We further showed how option prices evolve when varying certain model parameters. An empirical study was also carried out to demonstrate the model performance if it was to be applied in practice.

Keywords: Heston-Vasicek model; regime switching factor; analytical pricing formula; European options
Mathematics Subject Classification: 91G20

1. Introduction

In 1973, Black and Scholes [5] introduced a groundbreaking formula used to value European options, assuming a normal distribution for logarithmic asset returns. This model, while widely acclaimed [21,58], has faced significant challenges, primarily due to the overly simplistic assumptions made to facilitate analytical solutions. One such limitation is assumed constant volatility, which contradicts real market behavior, particularly the "volatility smile" effect [16]. This discrepancy has spurred extensive research aimed at refining or adjusting the Black-Scholes framework to better reflect actual market dynamics.

Stochastic volatility models have become widely adopted by incorporating volatility as an additional random process alongside the asset price. While this adjustment more accurately captures the variability of volatility over time, it complicates the option pricing problem significantly. In many cases, maintaining analytical tractability is no longer feasible, necessitating the use of numerical methods [35, 46, 52]. However, these numerical techniques are often impractical due to their high computational demands and the time-consuming process of model calibration, particularly in the context of modern algorithmic trading. As a result, there is a strong push within the research community to develop stochastic volatility models that retain analytical solvability.

When volatility is modeled as a geometric Brownian motion, prices of European options are expressed as a power series [31], assuming the uncorrelated underlying-volatility relationship. However, this assumption contradicts the observed "leverage effect", which suggests a negative correlation between the two [3]. Alternatively, when volatility follows an Ornstein-Uhlenbeck process [45, 49], analytical solutions for European options are possible, though this approach has the drawback of allowing negative volatility values. A key breakthrough in volatility modeling was achieved by Heston [29], who introduced the use of a Cox-Ingersoll-Ross (CIR) process for stochastic volatility. This formulation ensures the non-negativity of volatility while capturing the mean-reverting dynamics empirically observed in financial markets [4]. Heston's model provides a closed-form pricing solution for European options, facilitating efficient calibration. As a result of the Heston model's effectiveness, there have been extensive applications in valuing financial derivatives [6, 19, 55].

However, stochastic volatility models, including the Heston model, are often limited in their ability to fully capture underlying dynamics. To enhance the flexibility in fitting real market data, more advanced modeling approaches have been developed. A notable example is the time-varying Heston model, where its constant parameters are allowed to change over time [42]. Additionally, multi-factor stochastic volatility models have gained popularity [27,41,48], as these models are better at describing volatility smile [13]. Another recent development in derivative pricing is the use of Markov-modulated models [8], which are empirically inspired by actual market behaviors [24]. Regime switching has even been integrated into the Heston framework [18, 28], as it improves the predictive power of stochastic volatility models and helps account for significant market events, as noted by Vo [50]. More recently, combining regime switching with multi-factor stochastic volatility models has emerged as a promising approach, benefiting from the strengths of both frameworks in modeling asset dynamics [30, 39]. Recently, the persistence and roughness of volatility have prompted the development of various rough volatility models [20, 51].

Apart from stochastic volatility models, relaxing the assumption of a constant interest rate in the Black-Scholes framework is also important. Research has shown that incorporating a stochastic interest rate helps to improve the degree of fitness significantly [1], which has given rise to various hybrid models combining both stochastic volatility and stochastic interest rates. However, integrating a Heston-type volatility model with a stochastic interest rate presents a challenge: when the interest rate is correlated with the underlying asset price, analytical pricing formulas are not available [2], and only approximation methods can be used [10,22,23,56]. Closed-form solutions for these hybrid models are only possible when the interest rate and asset price are assumed to be independent [40, 53, 57].

This paper introduces a novel two-factor hybrid model, where the volatility factors are driven by the Heston process and a Markov chain, and the interest rate evolves according to the Vasicek model. Although incorporating these three elements increases the model's complexity, we can still

value European options analytically. This is achieved by working out the underlying logarithmic characteristic function, leveraging the numeraire change technique and the tower rule of expectation. A key advantage of our approach is that it preserves analytical tractability, even with the correlation between underlying and interest rate. To showcase our model's effectiveness, we perform numerical simulations to analyze the behavior of the pricing formula and present empirical results based on real data, highlighting our model's superiority compared to existing alternatives. Note that in our framework, the short rate is correlated solely with the regime-switching volatility component, not with the Heston-type variance factor. This simplification is necessary to derive a closed-form characteristic function. Despite this specific correlation structure, the model still captures a key channel of equity-interest rate dependence. This feature also distinguishes our model from those in the literature [11,53], which do not incorporate stochastic interest rates or explicit equity-rate dependence.

This paper is organized as follows. Section 2 outlines the proposed two-factor Heston-Vasicek hybrid model. In Section 3, we derive a general pricing formula for European options, initially involving an unknown characteristic function, which is subsequently determined using the conditional characteristic function, assuming full knowledge of the Markov chain's information. Section 4 presents numerical examples along with a discussion of the results. Section 5 features an empirical analysis, and the final section offers concluding remarks.

2. The two-factor Heston-Vasicek hybrid model

We work on a filtered probability space $(\Omega, \mathcal{F}, \{\mathcal{F}_t\}_{t\geq 0}, \mathbb{Q})$, where the filtration $\{\mathcal{F}_t\}$ is generated by the Brownian motions $\{W^S_{1,t}, W^S_{2,t}, W^v_t, W^r_t\}$ and the continuous-time Markov chain X_t, augmented with the $\mathbb{Q}$-null sets. The following structural assumptions are made throughout the paper.

1. The Brownian motions $\{W^S_{1,t}, W^S_{2,t}, W^v_t, W^r_t\}$ and the Markov chain X_t are mutually independent.
2. The variance process v_t follows CIR dynamics under $\mathbb{Q}$; to ensure its positivity, we assume the Feller condition $2k\theta \geq \sigma^2$ holds. If the condition is violated, the SDE (stochastic differential equation) remains well-defined and the model can still be used in practice, as is common in the Heston literature.
3. The Vasicek short-rate process r_t allows for negative interest rates, which is not only mathematically convenient but also empirically relevant in the post-2008 and post-pandemic financial environment, where several major economies have experienced periods of negative nominal rates.
4. The regime-switching volatility factor ξ_{X_t} is a piecewise-constant process modulated by X_t; it does not possess its own diffusion dynamics.
5. The correlation structure is restricted as follows:

$$dW^S_{1,t}dW^v_t = \rho_1 dt, \quad dW^S_{2,t}dW^r_t = \rho_2 dt,$$

   while all other pairwise correlations are zero.
6. All model coefficients are adapted to $\{\mathcal{F}_t\}$ and satisfy suitable integrability conditions for the SDEs and the characteristic function to be well-defined.

The model involves the following parameters in Table 1, which will be kept fixed unless stated otherwise in numerical examples and empirical analysis.

Table 1. Model parameters and their meanings.

Symbol	Meaning	Typical domain
k	speed of mean reversion of v_t	$k > 0$
θ	long-run level of v_t	$\theta > 0$
σ	volatility of volatility	$\sigma > 0$
α	speed of mean reversion of r_t	$\alpha > 0$
β	long-run level of r_t	$\beta \in \mathbb{R}$
η	volatility of r_t	$\eta > 0$
ρ_1	correlation between W^{S_1} and W^v	$-1 \le \rho_1 \le 1$
ρ_2	correlation between W^{S_2} and W^r	$-1 \le \rho_2 \le 1$
v_0	initial variance	$v_0 > 0$
r_0	initial short rate	$r_0 \in \mathbb{R}$
ξ_i	volatility level in regime i ($i = 1, \ldots, N$)	$\xi_i \ge 0$
λ_{ij}	transition intensity from regime i to j	$\lambda_{ij} \ge 0$

We now introduce the two-factor Heston-Vasicek hybrid model, where both volatility and interest rates are treated as stochastic processes. The volatility is modeled using two components: one driven by a CIR process and the other governed by regime switching, while the interest rate follows an Ornstein-Uhlenbeck process. It should be pointed out that this is not a "two-factor Heston model" in the usual sense, where two independent CIR-type variance factors are assumed. Instead, the second factor is a Markov-modulated constant that captures discrete shifts in volatility levels. This choice is financially motivated by the observation that volatility regimes often persist over medium-term horizons, and it allows us to maintain analytical tractability while still capturing regime-dependent smile patterns. To establish the connection between the proposed two-factor model and existing approaches, we begin by outlining the classical one-factor Heston-Vasicek model under the risk-neutral measure $\mathbb{Q}$:

$$\begin{aligned} \frac{dS_t}{S_t} &= r_t dt + \sqrt{v_t} dW^S_{1,t}, \\ dv_t &= k(\theta - v_t)dt + \sigma\sqrt{v_t} dW^v_t, \\ dr_t &= \alpha(\beta - r_t)dt + \eta dW^r_t. \end{aligned} \tag{2.1}$$

Here, S_t represents the underlying asset price. Note that W^r_t is assumed to be independent of the other two to maintain analytical tractability. Consequently, to account for the asset-interest relationship, a two-factor model is naturally adopted, as described below.

$$\begin{aligned} \frac{dS_t}{S_t} &= r_t dt + \sqrt{v_t} dW^S_{1,t} + \xi dW^S_{2,t}, \\ dv_t &= k(\theta - v_t)dt + \sigma\sqrt{v_t} dW^v_t, \\ dr_t &= \alpha(\beta - r_t)dt + \eta dW^r_t, \end{aligned} \tag{2.2}$$

with the second factor of the volatility being a constant ξ.

As previously noted, empirical studies have provided substantial evidence of regime-switching behavior in actual markets [24]. To incorporate this feature into our model, we introduce a continuous-time Markov chain with a finite set of states $X_t \in \{e_1, e_2, ..., e_N\}$, which operates independently of the four Brownian motions. Each e_i represents a unit vector in the N-dimensional space, where

the i-th component is equal to one. This structure, according to the semi-martingale representation theorem [17], can be expressed as follows:

$$X_t = X_0 + \int_0^t \Lambda(s) X_s ds + L_t, \tag{2.3}$$

with $\Lambda(t) = [\lambda_{ij}(t)]_{i,j=1,2,...,N}$ being its generating matrix. L_t is a martingale increment process. We further assume that the second factor of the volatility is regime switching, i.e., rather than remaining fixed, ξ_{X_t} is now permitted to transition between various states according to the behavior of the Markov chain. Thus, model dynamics evolve to reflect these state-dependent changes, as described by the following formulation:

$$\begin{aligned} \frac{dS_t}{S_t} &= r_t dt + \sqrt{v_t} dW_{1,t}^S + \xi_{X_t} dW_{2,t}^S, \\ dv_t &= k(\theta - v_t)dt + \sigma\sqrt{v_t} dW_t^v, \\ dr_t &= \alpha(\beta - r_t)dt + \eta dW_t^r. \end{aligned} \tag{2.4}$$

Here, we have $\xi_{X_t} = \ < \bar{\xi}, X_t >, \bar{\xi} = (\xi_1, \xi_2, ..., \xi_N)^T$ if we assume that $< \cdot, \cdot >$ represents two vectors' inner product, and for each t, ξ_{X_t} produces a scalar value.

By incorporating a second regime-switching component for volatility and considering the asset-interest correlation, a key question arises: Can we maintain analytical tractability? Analytical pricing formulas are highly valuable in practice, so addressing this issue is crucial. A thorough discussion of this matter is presented in the following section.

3. European option pricing

This section introduces a general formula for evaluating European call options through the application of measure transformation. Following this, under the forward measure, the underlying logarithmic characteristic function is derived, ensuring that the resulting formula is both fully analytical and exact.

3.1. The general pricing approach

One can use

$$U(S, v, r, X_t, t) = E^{\mathbb{Q}}\left[e^{-\int_t^T r(s)ds} \max(S_T - K, 0) | S_t, v_t, r_t, X_t\right] \tag{3.1}$$

to compute the value of a European call. The formula can be further simplified as

$$U(S, v, r, X_t, t) = P(r, t, T) E^{\mathbb{Q}^T}\left[\max(S_T - K, 0) | S_t, v_t, r_t, X_t\right]. \tag{3.2}$$

Here, $\mathbb{Q}^T$ is the T-forward measure. $P(r, t, T)$ represents bond prices under $\mathbb{Q}$ expiring at T with no coupon, and its formula can be straightforwardly derived according to the results in [27]:

$$P(r, t, T) = e^{A(\tau) - B(\tau)r}, \ \tau = T - t, \tag{3.3}$$

with

$$A(\tau) = \left(\frac{\eta^2}{2\alpha^2} - \beta\right)\tau + \frac{1}{\alpha}\left(\frac{\eta^2}{\alpha^2} - \beta\right)(e^{-\alpha\tau} - 1) - \frac{\eta^2}{4\alpha^2}\left(e^{-2\alpha\tau} - 1\right),$$

$$B(\tau) = \frac{1}{\alpha}\left(1 - e^{-\alpha\tau}\right).$$

One should expect that the expectation involved in (3.2) needs to be computed before obtaining an analytical pricing formula. Since we take expectations under $\mathbb{Q}^T$, the first step is to determine the dynamics under this forward measure.

To apply the measure transform technique, we introduce four independent Brownian motions $W^{\mathbb{Q}}_{1,t}$, $W^{\mathbb{Q}}_{2,t}$, $W^{\mathbb{Q}}_{3,t}$, and $W^{\mathbb{Q}}_{4,t}$ as

$$\begin{bmatrix} dW^S_{1,t} \\ dW^S_{2,t} \\ dW^v_t \\ dW^r_t \end{bmatrix} = C \times \begin{bmatrix} dW^{\mathbb{Q}}_{1,t} \\ dW^{\mathbb{Q}}_{2,t} \\ dW^{\mathbb{Q}}_{3,t} \\ dW^{\mathbb{Q}}_{4,t} \end{bmatrix}, \tag{3.4}$$

where the correlation matrix C is

$$C = \begin{bmatrix} 1 & 0 & 0 & 0 \\ 0 & 1 & 0 & 0 \\ \rho_1 & 0 & \sqrt{1-\rho_1^2} & 0 \\ 0 & \rho_2 & 0 & \sqrt{1-\rho_2^2} \end{bmatrix}. \tag{3.5}$$

With

$$\mu^{\mathbb{Q}} = \begin{bmatrix} r_t \\ k(\theta - v_t) \\ \alpha(\beta - r_t) \end{bmatrix}, \quad \Sigma = \begin{bmatrix} \sqrt{v_t} & \xi_{X_t} & 0 & 0 \\ 0 & 0 & \sigma\sqrt{v_t} & 0 \\ 0 & 0 & 0 & \eta \end{bmatrix}, \tag{3.6}$$

we can alternatively represent our model dynamics as

$$\begin{bmatrix} \dfrac{dS_t}{S_t} \\ dv_t \\ dr_t \end{bmatrix} = \mu^{\mathbb{Q}}dt + \Sigma \times C \times \begin{bmatrix} dW^{\mathbb{Q}}_{1,t} \\ dW^{\mathbb{Q}}_{2,t} \\ dW^{\mathbb{Q}}_{3,t} \\ dW^{\mathbb{Q}}_{4,t} \end{bmatrix}. \tag{3.7}$$

With a systematic expression of the model dynamics as presented in (3.7), one can compute $\mu^{\mathbb{Q}^T}$ using the theory in [7]:

$$\mu^{\mathbb{Q}^T} = \mu^{\mathbb{Q}} - \Sigma \times \left(CC^T\right) \times \left(\frac{\sigma^{N_{1,t}}}{N_{1,t}} - \frac{\sigma^{N_{2,t}}}{N_{2,t}}\right), \tag{3.8}$$

if under $\mathbb{Q}$ and $\mathbb{Q}^T$, $\sigma^{N_{1,t}}$ and $\sigma^{N_{2,t}}$ respectively denote the numeraires' volatility terms with respect to the original correlated Brownian vector [7, 9]. Clearly, the derivation of μ^{Q^T} needs to represent the two numeraires, the definitions of which are

$$N_{1,t} = e^{\int_0^t r(s)ds}, \; N_{2,t} = P(r,t,T).$$

Thus, one could easily present

$$dN_{1,t} = N_{1,t}r(t)dt,$$

$$dN_{2,t} = N_{2,t}\left\{\left[\frac{dA}{dt} - \frac{dB}{dt}r - \alpha(\beta - r)B + \frac{1}{2}\eta^2 B^2\right]dt - \eta B dW_t^r\right\},$$

implying that $\sigma^{N_{1,t}}$ is a four-dimensional column zero vector, and $\sigma^{N_{2,t}}$ is also a column vector with its first three entries being 0 and the last one being $-\eta B N_{2,t}$. This provides

$$\begin{aligned}\mu^{\mathbb{Q}^T} &= \begin{bmatrix} r_t \\ k(\theta - v_t) \\ \alpha(\beta - r_t) \end{bmatrix} - \begin{bmatrix} \sqrt{v_t} & \xi_{X_t} & 0 & 0 \\ 0 & 0 & \sigma\sqrt{v_t} & 0 \\ 0 & 0 & 0 & \eta \end{bmatrix} \times \begin{bmatrix} 1 & 0 & \rho_1 & 0 \\ 0 & 1 & 0 & \rho_2 \\ \rho_1 & 0 & 1 & 0 \\ 0 & \rho_2 & 0 & 1 \end{bmatrix} \times \begin{bmatrix} 0 \\ 0 \\ 0 \\ \eta B \end{bmatrix} \\ &= \begin{bmatrix} (r_t - \rho_2\eta\xi_{X_t}B) \\ k(\theta - v_t) \\ \alpha\beta - B\eta^2 - \alpha r_t \end{bmatrix}. \end{aligned} \tag{3.9}$$

We now finish the measure transformation by presenting underlying dynamics under $\mathbb{Q}^T$:

$$\begin{bmatrix} \frac{dS_t}{S_t} \\ dv_t \\ dr_t \end{bmatrix} = \begin{bmatrix} (r_t - \rho_2\eta\xi_{X_t}B) \\ k(\theta - v_t) \\ \alpha\beta - B\eta^2 - \alpha r_t \end{bmatrix} dt + \Sigma \times C \times \begin{bmatrix} dW_{1,t}^{\mathbb{Q}^T} \\ dW_{2,t}^{\mathbb{Q}^T} \\ dW_{3,t}^{\mathbb{Q}^T} \\ dW_{4,t}^{\mathbb{Q}^T} \end{bmatrix}. \tag{3.10}$$

To validate the measure transform, we need to check whether $\frac{S_t}{P(r_t,t,T)}$ is a $\mathbb{Q}^T$-martingale. By applying the product rule of stochastic differentiation, we can derive

$$d\left[\frac{S_t}{P(r_t,t,T)}\right] = \tilde{P}(r_t,t,T)dS_t + S_t d\tilde{P}(r_t,t,T) + dS_t d\tilde{P}(r_t,t,T),$$

where $\tilde{P}(r_t,t,T) = \frac{1}{P(r_t,t,T)} = e^{B(\tau)r - A(\tau)}$. Applying Ito's lemma further yields

$$\begin{aligned} d\tilde{P}(r_t,t,T) &= \tilde{P}(r_t,t,T)\left\{\left[\frac{dB}{dt}r - \frac{dA}{dt} + B(\alpha\beta - B\eta^2 - \alpha r) + \frac{1}{2}B^2\eta^2\right]dt \right. \\ &+ \left. B\eta\left(\rho_2 dW_{2,t}^{\mathbb{Q}^T} + \sqrt{1-\rho_2^2}dW_{4,t}^{\mathbb{Q}^T}\right)\right\}. \end{aligned}$$

Thus, one can obtain

$$d\left[\frac{S_t}{P(r_t,t,T)}\right] = \mu^{S/P}dt + \sqrt{v_t}dW_{1,t}^{\mathbb{Q}^T} + \xi_{X_t}dW_{2,t}^{\mathbb{Q}^T} + B\eta\left(\rho_2 dW_{2,t}^{\mathbb{Q}^T} + \sqrt{1-\rho_2^2}dW_{4,t}^{\mathbb{Q}^T}\right),$$

where

$$\mu^{S/P} = \left(\frac{dB}{dt} - \alpha B + 1\right)r + \alpha\beta B - \frac{1}{2}B^2\eta^2 - \frac{dA}{dt}.$$

Since B and A satisfy [27]

$$\begin{aligned} \frac{dB}{dt} &= \alpha B - 1, \\ \frac{dA}{dt} &= \alpha\beta B - \tfrac{1}{2}B^2\eta^2, \end{aligned}$$

we must have $\mu^{S/P} = 0$, which indicates that $\dfrac{S_t}{P(r_t, t, T)}$ is a $\mathbb{Q}^T$-martingale.

Let $y_t = \ln(S_t)$. The general formula (3.2) can thus be reformulated as

$$U(y, v, r, X_t, t) = P(r, t, T)\,(P_1 - KP_2)\,, \tag{3.11}$$

where

$$P_1 = \int_{\ln K}^{+\infty} e^{y_T} p(y_T) dy_T,\ P_2 = \int_{\ln K}^{+\infty} p(y_T) dy_T.$$

Under $\mathbb{Q}^T$, $p(y_t)$ is the density of y_t, whose characteristic function, with $j = \sqrt{-1}$, can be defined by

$$f(\phi; t, T, y_t, v_t, r_t, X_t) = E^{Q^T}\left(e^{j\phi y_T} | y_t, v_t, r_t\right) = \int_{-\infty}^{+\infty} e^{j\phi y_T} p(y_T) dy_T.$$

Setting $\phi = -j$ in the above equation yields

$$f(-j; t, T, y_t, v_t, r_t, X_t) = \int_{-\infty}^{+\infty} e^{y_T} p(y_T) dy_T.$$

Both sides of this equation, if divided by $f(-j; t, T, y_t, v_t, r_t, X_t)$, produce

$$\int_{-\infty}^{+\infty} \frac{e^{y_T} p(y_T)}{f(-j; t, T, y_t, v_t, r_t, X_t)} dy_T = 1.$$

Thus, it is straightforward that

$$P_1 = f(-j; t, T, y_t, v_t, r_t, X_t)\left\{\frac{1}{2} + \frac{1}{\pi}\int_0^{+\infty} Real\left[\frac{e^{-j\phi \ln K} f(\phi - j; t, T, y_t, v_t, r_t, X_t)}{j\phi f(-j; t, T, y_t, v_t, r_t, X_t)}\right] d\phi\right\}. \tag{3.12}$$

Of course, P_2 can be directly simplified as

$$P_2 = \frac{1}{2} + \frac{1}{\pi}\int_0^{+\infty} Real\left[\frac{e^{-j\phi \ln K} f(\phi; t, T, y_t, v_t, r_t, X_t)}{j\phi}\right] d\phi. \tag{3.13}$$

It should be remarked that we require $-1 \le \rho_1, \rho_2 \le 1$ for the formulae (3.12) and (3.13) to be valid, and the inversion integrals are taken along lines in the complex plane where the integrand is integrable.

After completing all of these steps, the pricing formula now contains the characteristic function f under $\mathbb{Q}^T$ as the only unknown term, solving which would yield the final analytical pricing formula, and the details are provided in the next subsection.

3.2. The characteristic function

The characteristic function derivation procedure is broken down into two steps. In the first step, it is assumed that all information about the Markov chain up to the maturity time is available at the present time, leading to the formulation of a conditional characteristic function. One should then proceed to the second step to find the expected value of this intermediate result.

Let us first fix a realization of the Markov chain path $\{X_s, t \le s \le T\}$, denoted by x_s, and define the conditional characteristic function

$$h(\phi; t, T, y_t, v_t, r_t, x_s) = E^{\mathbb{Q}^T}\left(e^{j\phi y_T} | y_t, v_t, r_t, x_s\right).$$

Then, h satisfies the following PDE:

$$\begin{aligned}\frac{\partial h}{\partial \tau} &= \left(\frac{1}{2}v+\frac{1}{2}\xi_t^2\right)\frac{\partial^2 h}{\partial y^2}+\frac{1}{2}\sigma^2 v\frac{\partial^2 h}{\partial v^2}+\frac{1}{2}\eta^2\frac{\partial^2 h}{\partial r^2}+\rho_1\sigma v\frac{\partial^2 h}{\partial y\partial v}+\rho_2\eta\xi_t\frac{\partial^2 h}{\partial y\partial r}\\ &+ \left(r_t-\rho_2\eta\xi_t B-\frac{1}{2}v-\frac{1}{2}\xi_t^2\right)\frac{\partial h}{\partial y}+k(\theta-v)\frac{\partial h}{\partial v}+\left(\alpha\beta-B\eta^2-\alpha r\right)\frac{\partial h}{\partial r},\end{aligned} \tag{3.14}$$

with the initial condition $h|_{\tau=0}=e^{j\phi y_t}$. As we assume here that the path x_s is pre-given, ξ_{X_t} is no longer random, but just time dependent, producing a scalar value for each time moment t, and we have thus denoted it as ξ_t. In this case, following much of the existing literature [12, 26, 29, 38, 43], we denote $\tau=T-t$, and the substitution of

$$h=e^{G(\phi;\tau)+D(\phi;\tau)v_t+E(\phi;\tau)r_t+j\phi y_t} \tag{3.15}$$

into PDE (3.14) yields

$$\begin{aligned}\frac{dD}{d\tau} &= \frac{1}{2}\sigma^2D^2+(j\phi\rho_1\sigma-k)D-\frac{1}{2}(j\phi+\phi^2),\ D(\phi;0)=0,\\ \frac{dE}{d\tau} &= j\phi-\alpha E,\ E(\phi;0)=0,\\ \frac{dG}{d\tau} &= \frac{1}{2}\eta^2E+k\theta D+(\alpha\beta-\eta^2B)E+j\phi\rho_2\eta\xi_t(E-B)-\frac{1}{2}(j\phi+\phi^2)\xi_t^2,\ G(\phi;0)=0.\end{aligned}$$

$D(\phi;\tau)$ solves a Riccati equation whose coefficients are constant, and one can write its solution as:

$$D=\frac{d-(j\phi\rho_1\sigma-k)}{\sigma^2}\cdot\frac{1-e^{d\tau}}{1-ge^{d\tau}}, \tag{3.16}$$

with

$$d=\sqrt{(j\phi\rho_1\sigma-k)^2+\sigma^2(j\phi+\phi^2)},\ g=\frac{(j\phi\rho_1\sigma-k)-d}{(j\phi\rho_1\sigma-k)+d}.$$

$E(\phi;\tau)$ satisfies a first-order linear ODE, and one can apply the general solution to derive

$$E(\phi;\tau)=\frac{j\phi}{\alpha}(1-e^{-\alpha\tau}). \tag{3.17}$$

As the terms on the right-hand side of the ODE governing $G(\phi;\tau)$ are all known by now, working out $G(\phi;\tau)$ just requires us to integrate its ODE directly, resulting in

$$G(\phi;\tau)=\bar{G}(\phi;\tau)+\tilde{G}(\phi;\tau), \tag{3.18}$$

with

$$\begin{aligned}\bar{G}(\phi;\tau) &= -\frac{\eta^2(\phi^2+2j\phi)}{2\alpha^2}\left[\tau-\frac{2}{\alpha}(1-e^{-\alpha\tau})+\frac{1}{2\alpha}(1-e^{-2\alpha\tau})\right]+\beta j\phi\left[\tau-\frac{1}{\alpha}(1-e^{-\alpha\tau})\right]\\ &+ \frac{k\theta}{\sigma^2}\left\{[d-(j\phi\rho_1\sigma-k)]\tau-2\ln\left(\frac{1-ge^{d\tau}}{1-g}\right)\right\},\end{aligned}$$

and

$$\tilde{G}(\phi;\tau) = (j\phi + \phi^2)\int_t^T -\frac{\rho_2\eta}{\alpha}\left[1 - e^{-\alpha(T-s)}\right] < \xi_s, X_s > -\frac{1}{2} < \xi_s^2, X_s > ds.$$

It should be remarked that when $\xi \equiv 0$ and $\rho_2 = 0$, one can easily find $\tilde{G}(\phi;\tau) = 0$, and $\bar{G}(\phi;\tau)$ is exactly the constant term of the characteristic function corresponding to the classical Heston-Vasicek hybrid model, which partially verifies the correctness of our derivation.

Once h has been successfully derived, the target characteristic function f can be calculated by applying the tower property of expectation:

$$f = e^{\bar{G}(\phi;\tau)+D(\phi;\tau)v_t+E(\phi;\tau)r_t+j\phi y_t} E^{\mathbb{Q}^T}\left(e^{\tilde{G}(\phi;\tau)}|X_t\right).$$

According to [18, Proposition 3.2], we can calculate the involved expectation as

$$E\left(e^{\tilde{C}(\phi;\tau)}|X_t\right) =< \left(e^{\Lambda^T\tau+Z}\right)X_t, I>. \tag{3.19}$$

Here, all elements of the N-dimensional vector I are equal to 1. $Z = \text{diag}\left[p(\phi;\tau)\bar{\xi} - \frac{1}{2}(j\phi+\phi^2)\bar{\xi}^2\tau\right]$, with

$$p(\phi;\tau) = -\frac{\rho_2\eta(j\phi+\phi^2)}{\alpha}\left[\tau - \frac{1}{\alpha}(1-e^{-\alpha\tau})\right].$$

The notation diag[·] refers to the diagonal matrix formed by placing a vector's elements along the main diagonal. Thus, we finally arrive at

$$f = e^{\bar{C}(\phi;\tau)+D(\phi;\tau)v_t+E(\phi;\tau)r_t+j\phi y_t} < \left(e^{\Lambda^T\tau+Z}\right)X_t, I>. \tag{3.20}$$

Based on the model dynamics described in (3.7), an analytical solution for European options can be formulated by combining Eqs (3.11) and (3.20). In the following section, numerical simulations are performed to explore European options' characteristics within our specific model, where the additional factor introduces regime switching.

4. Numerical experiments and discussions

In this section, our formula is validated numerically first to guarantee that no algebraic errors occurred when it was derived, and then the second regime-switching* factor's influence is demonstrated. Note that when implementing our formula, the integration over the Fourier variable was computed using the trapezoidal rule, with the truncation range as [0, 100] and the step size as 0.1. Unless otherwise stated in the following, the parameters are

$$\xi_1 = 0.01; \xi_2 = 0.1; \lambda_{12} = \lambda_{21} = 10; k = 10; \alpha = 5; \sigma = 0.1; \theta = 0.2; \beta = 0.1; \rho_1 = -0.8;$$
$$\rho_2 = -0.5; \eta = 0.05; r_0 = 0.03; v_0 = 0.1; S_0 = K = 100; \tau = 1; X_0 = (1,0)^T.$$

*We consider a two-state Markov chain in this section's numerical experiments and the next section's empirical analysis.

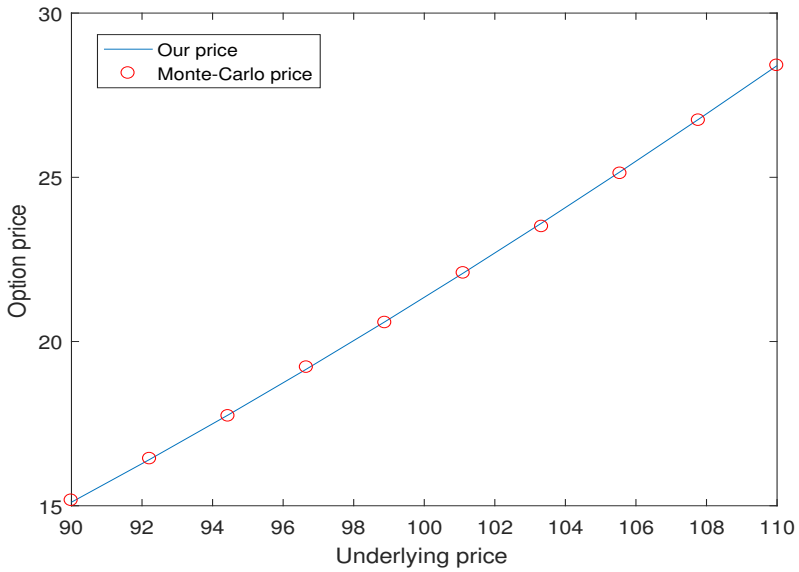

(a) Formula- and simulation-based prices.

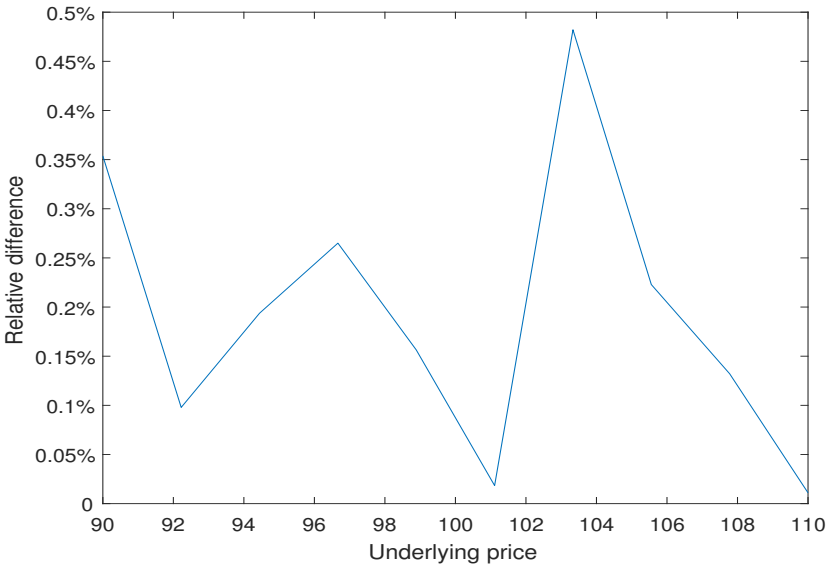

(b) Relative difference.

Figure 1. Accuracy verification.

Figure 1(a) presents the prices of European call options for State 1, as calculated using our analytical formula, alongside those obtained from direct Monte Carlo simulations by using a Euler scheme to exactly simulate the model dynamics with 500,000 sampling paths and the time discretization step 0.01. Both pricing methods exhibit an upward trend in relation to the underlying asset price, which aligns with typical financial intuition. It is also evident that the newly derived formula delivers highly accurate results, as the computed values closely match those from the Monte Carlo simulations. As demonstrated in Figure 1(b), their relative difference is bounded up by 0.5%, providing strong evidence

that our formula is reliable and suitable for practical implementation. Regarding computational performance, our approach computes an option price in approximately 0.07 seconds[†], which is over 400 times faster than the 28.36 seconds consumed by a standard Monte Carlo simulation for the same task. While this highlights the substantial efficiency of our method, we acknowledge that achieving the speed and stability required for real-time calibration in high-frequency trading may demand further refinement, a challenge we propose to address in future work.

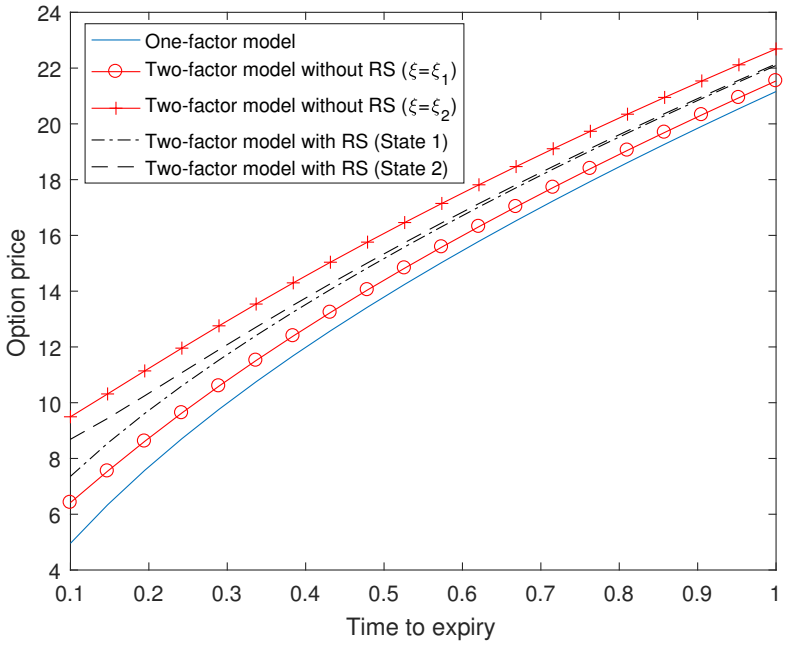

Figure 2. The difference among the three models.

Figure 2 provides a comparison of option prices generated by three distinct models: the traditional Heston-Vasicek hybrid model, its two-factor version without switching, and our proposed one considering regime switching. All models are implemented using identical parameter values. A key observation is that the option prices from the one-factor model are the lowest, which can be attributed to the absence of an additional volatility factor, resulting in lower risk and, consequently, a lower price. In contrast, the two-factor models incorporate additional volatility factors, which naturally increase both risk and price.

Our model's option prices for both states are higher than those from the two-factor model without regime switching when the second factor, ξ, is set to ξ_1. However, when ξ is set to ξ_2, our model's prices are lower. This difference arises because, in our model, the second factor switches between high and low values, whereas in the two-factor model without regime switching, the second factor is fixed throughout the option's life. Additionally, it is noteworthy that the price for State 1 in our model is consistently lower than that for State 2. This is due to the second factor in State 1 being smaller than in State 2. Furthermore, with an increase in time to maturity, the price gap of both states narrows, since a longer time to expiration allows the second factor to fluctuate more between its higher and lower

[†]All the results in this section are produced using MATLAB R2019b on a desktop with a 2.5 GHz Intel Core i5 CPU and 16 GB RAM.

values for States 1 and 2, respectively.

To further demonstrate the effects of the regime-switching mechanism, we set the two transition rates to be identical and illustrate in Figure 3 how the resultant option prices vary with changes in these rates. As anticipated, when the transition rates are set to zero, i.e., $\lambda_{12} = \lambda_{21} = 0$, the numerical option prices from our model align perfectly with those from the two-factor model without regime switching. This is because, in this scenario, regime switching does not occur in our model. As the transition rates increase, we observe that the option price for State 1 rises, while the price for State 2 decreases. This can be attributed to the fact that State 1 provides more possibility for higher volatility values, while smaller volatility values are more likely to be attained in State 2, influencing the respective option prices. It should also be noted that the rate of change for option prices of both states with respect to the transition rates are decreasing since larger transition rates imply more frequent regime switching, making the impact of the initial state of the second factor less significant on option prices. One can also observe that the regime-switching feature has larger impact on options with shorter maturities, where the volatility smile is more sensitive to regime shifts.

While the distinction between our model and the traditional Heston-Vasicek hybrid model is evident when using identical model parameters, this difference alone does not imply that our model will necessarily outperform the classical model when employing real data. In practice, model parameters must be calibrated based on actual market conditions. To address this, empirical results using SSE50ETF options are provided in the following section.

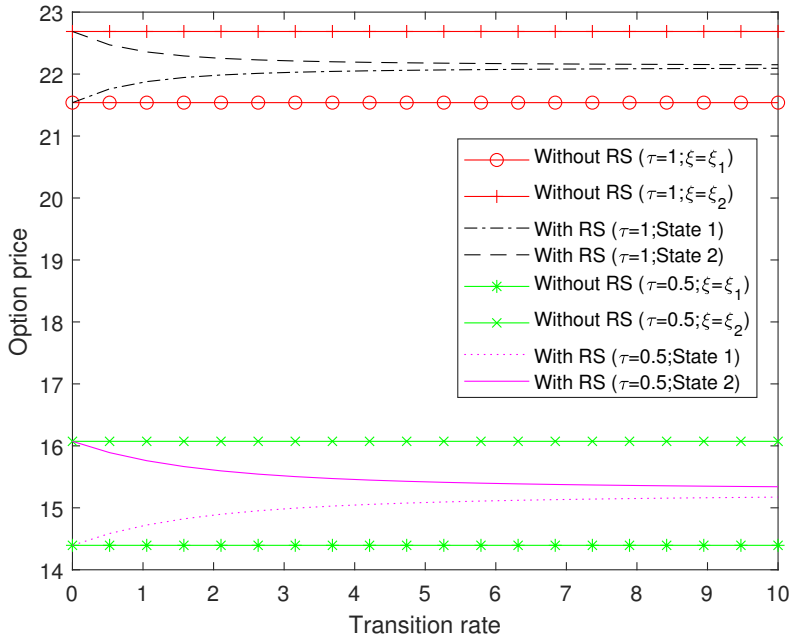

Figure 3. Option prices with respect to the transition rates.

5. Empirical studies

This section compares our newly proposed model's performance with the traditional Heston-Vasicek hybrid model to highlight the significance of including regime switching and the asset-interest

correlation. This comparison serves to demonstrate the added value of these factors in improving model accuracy. Before empirical results are presented in the last subsection, it is necessary to introduce the data set and the approach used for this empirical study, which forms the main content of the first and second subsections, respectively.

5.1. Data description

For calibrating both models, we use European options on the SSE50ETF from January to December 2023. Following several existing studies [3, 25], we rely exclusively on call options. While including both call and put options would offer a more comprehensive assessment of model performance, particularly in capturing volatility smiles/smirks, we leave this extension to future research. Note that this raw data is not used directly, as it is well recognized that unfiltered data often contains noise that can lead to inaccurate or misleading conclusions. Therefore, several data filtering techniques are applied to ensure the quality and reliability of the dataset.

Consistent with the approach in [3, 15] and other studies, we select only Wednesday option data for model calibration. Wednesday exhibits the lowest probability of being a public holiday and is less influenced by the "day-of-the-week" effect, making it a more reliable choice for analysis. Additionally, options with very short or long times to expiration are excluded, as those with fewer than 30 days or over 90 days to maturity tend to exhibit high price volatility or inflated premiums, which can distort results [37]. Furthermore, options that are deeply in-the-money or deeply out-of-money are removed due to their association with liquidity issues [47]. Specifically, options with an absolute moneyness greater than 10%, with moneyness calculated as $(S - K)/K$.

After applying these filters, we obtain approximately 20–40 options per Wednesday, with a total of 1240 option quotes across the 48 calibration dates. The resulting dataset is ready for parameter estimation. To determine the model parameters, an appropriate method must be selected, which is explained in detail below.

5.2. Parameter estimation

The process of determining model parameters involves identifying the "optimal" set that ensures the model-generated option prices closely match those observed in the real market. This can be framed as an optimization problem, where the goal is to minimize the discrepancy between the model's prices and the actual market prices. If N refers to the observed number in one estimation, C_{Market} represents one observed option price in the market, and C_{model} denotes the price predicted by the model. A commonly used approach to achieve this is by minimizing the dollar mean-squared error (MSE) [14, 54]:

$$MSE = \frac{1}{N}\sum_{i=1}^{N}\left(C_{Market} - C_{Model}\right)^2. \tag{5.1}$$

To minimize Eq (5.1), an appropriate optimization technique must be employed. These techniques generally fall into two main categories: local and global optimization. Local optimization methods are relatively straightforward and quick to implement but are often criticized for getting trapped in local minima, which is a concern in our case, as multiple local minima may exist when minimizing (5.1) since it is not convex. On the other hand, global optimization methods, which incorporate stochastic

elements in the search process, are better equipped to avoid local minima and are therefore commonly preferred when calibrating option pricing models.

Simulated annealing (SA) [36] has received a lot of attention among global optimization approaches ever since it was proposed due to its remarkable advantages. In addition to being simple to implement and having minimal parameters that need adjustment, it also offers a theoretical assurance of converging to the global minimum. This is a highly desirable characteristic, as it guarantees that the global minimum can be reached. However, the SA converges very slowly, posing an obstacle for its practical applications, and various modifications to the SA have thus been proposed. What we adopt here is one of its well-known variations, the so-called adaptive simulated annealing (ASA) [32]. The ASA algorithm offers significant improvements over the traditional SA [34]. It is not only more efficient but also less reliant on user-defined parameters, making it a more robust approach. The widespread use of ASA across various fields, such as model calibration [42,44], highlights its growing popularity and versatility.

The ASA can be implemented using the open-source code available in [33], offering increased flexibility and enhanced capabilities through ongoing user feedback. We summarize the calibrated parameter bounds and their daily averaged estimates in Table 2. In executing the ASA algorithm, we employ 10 restarts to avoid local minima and ensure the robustness of the optimization.

Table 2. Parameter bounds and estimated results.

	Lower bound	Upper bound	Ours	Heston-Vasicek model
k	0	20	6.3870	13.6140
θ	0	1	0.0866	0.0121
σ	0	5	2.5205	2.1216
α	0	20	12.2883	13.9418
β	-1	1	0.0824	0.1055
η	0	5	1.9487	2.2573
ρ_1	-1	1	-0.1398	-0.0683
ρ_2	-1	1	-0.0823	
v_0	0	1	0.0137	0.0383
ξ_1	0	1	0.0174	
ξ_2	0	1	0.1672	
λ_{12}	0	20	7.2033	
λ_{21}	0	20	7.9157	

$\xi_1, \xi_2, \lambda_{12}$, and λ_{21}, are shown in Figure 4, and exhibit meaningful variation without erratic instability over the sample period. The low-volatility regime parameter ξ_1 remains relatively stable at low levels, while the high-volatility regime parameter ξ_2 shows considerable fluctuations, often reaching values an order of magnitude larger than ξ_1. Both transition intensities λ_{12} and λ_{21} vary substantially across dates, reflecting shifts in the frequency of regime transitions. This pattern supports the economic interpretation of the model capturing distinct volatility regimes with time-varying persistence, and indicates that the additional parameters are well-identified and stable enough for practical use.

Following the estimation, the performance of both models on this specific dataset can be evaluated, and the results will be discussed in the following subsection.

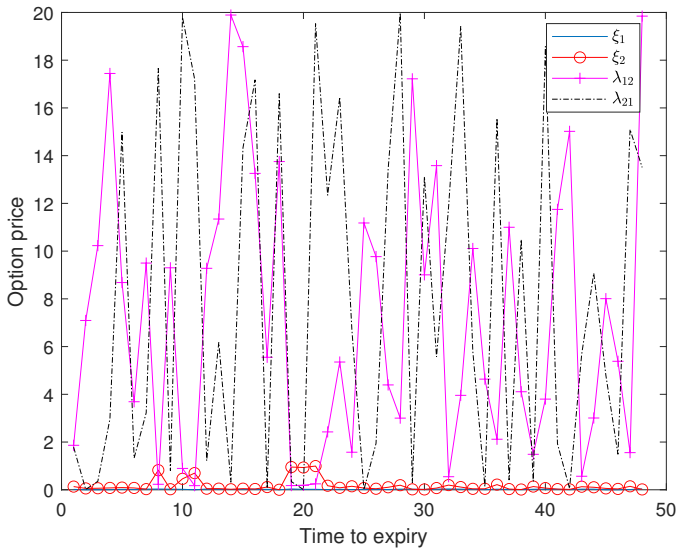

Figure 4. The additional parameters introduced by regime switching.

5.3. Empirical comparison

Since the model calibration involves minimizing the discrepancy between the market and model prices of the options used for parameter estimation, it is logical to consider the residual value of Eq (5.1) in this context, which is also named as the "in-sample error", after model calibration to show the model performance, since its magnitude measures the closeness between the two prices. On the other hand, a different measure of the model's performance can be assessed through the "prediction error" or "out-of-sample error". This is computed using Eq (5.1), which compares the market prices from a separate dataset with the model ones generated from the calibrated parameters. Data from Thursday is utilized for this evaluation. Table 3 presents both models' daily averaged in-sample and out-of-sample errors, both in terms of MSE and MAPE (mean absolute percentage error), defined as $\frac{|C_{Market} - C_{Model}|}{C_{Market}}$.

Table 3. Both models' pricing errors.

	Ours	Heston-Vasicek model
In-sample MSE	3.46E-6	4.31E-6
In-sample MAPE	1.14E-2	1.43E-2
Out-of-sample MSE	4.89E-5	1.18E-4
Out-of-sample MAPE	5.50E-2	6.95E-2

Table 2 reports the in-sample and out-of-sample pricing errors of the proposed model and the benchmark Heston-Vasicek model. The results indicate that our model consistently achieves lower errors across all metrics. For in-sample performance, our model yields an MSE of 3.46E-6 and an MAPE of 1.14E-2, compared to 4.31E-6 and 1.43E-2 for the Heston-Vasicek model, reflecting an improvement in both accuracy measures. More notably, in out-of-sample tests, the superiority of our model becomes even more pronounced: Our MSE (4.89E-5) is less than half of that of the Heston-Vasicek model (1.18E-4), and our MAPE (5.50E-2) is substantially lower than the benchmark's 6.95E-

2. These results demonstrate that the proposed model not only fits the historical data more closely but also generalizes better to unseen data, offering enhanced pricing accuracy and robustness.

To further assess model performance, we categorize options into three moneyness groups: In-the-money (ITM, $[0.03, 0.1]$), at-the-money (ATM, $[-0.03, 0.03]$), and out-of-the-money (OTM, $[-0.1, -0.03]$). The out-of-sample errors across these categories are reported in Table 4. Overall, the proposed model yields consistently lower MSE and MAPE values than the Heston-Vasicek benchmark in all moneyness segments. The improvement is most pronounced for OTM options, where the MSE is reduced by 74.9%. A similarly substantial reduction of 69.6% is observed for ATM options. In terms of MAPE, the proposed model also outperforms the benchmark across all categories, with the strongest relative improvement, an 18.9% decrease, occurring in the ATM group. These findings suggest that the proposed model not only enhances pricing accuracy uniformly but is particularly effective in the OTM and ATM regions, where conventional models tend to exhibit larger pricing deviations.

Table 4. Out-of-sample errors in different moneyness categories.

Moneyness		OTM	ATM	ITM
Ours	MSE	2.94E-5	4.04E-5	5.81E-5
	MAPE	1.34E-1	5.22E-2	1.94E-2
Heston-Vasicek model	MSE	1.17E-4	1.33E-4	1.02E-4
	MAPE	1.59E-1	6.44E-2	2.31E-2
Number of observations		361	501	752

To examine performance across the contract horizon, we partition the sample into two maturity groups: Short-term (time to maturity $\leq$ 60 days) and long-term (time to maturity $>$ 60 days). The corresponding out-of-sample errors are presented in Table 5. Overall, the proposed model outperforms the Heston-Vasicek benchmark in both maturity segments across MSE and MAPE metrics. The improvement is especially marked for long-term options, where the MSE is reduced by 57.6%. For short-term options, the reduction in MSE is more moderate at 19.7%. In terms of MAPE, the proposed model also achieves lower errors in both groups, with a noticeable reduction of 30.6% in the long-term category. These results indicate that the proposed model delivers robust pricing accuracy across maturities, while offering particularly substantial error reduction for longer-dated options, where the benchmark model tends to exhibit larger deviations.

Table 5. Out-of-sample errors in different maturity categories.

Time to maturity		$\leq$ 60 days	$>$ 60 days
Ours	MSE	1.39E-5	7.72E-5
	MAPE	4.70E-2	5.06E-2
Heston-Vasicek model	MSE	1.73E-5	1.82E-4
	MAPE	4.78E-2	7.29E-2
Number of observations		893	721

6. Conclusions

This study explores the combined effects of multi-factor stochastic volatility, regime switching, and stochastic interest rates by integrating the Vasicek model for interest rates with a two-factor stochastic volatility model. In this framework, the volatility dynamics are governed by a continuous-time Markov chain and the Heston model. With the Markov chain being predefined, we derive the underlying logarithmic conditional characteristic function, from which the unconditional one is obtained, leading to an analytical formulation of European options. The accuracy of this new formula is validated through numerical experiments, which also highlight the significant influence of the second regime-switching volatility factor on option pricing. Our results empirically confirm that across the tested data set, the proposed model performs better over the classical one-factor model, suggesting that it could serve as a strong alternative to the Heston-Vasicek framework in practical applications.

Author contributions

Xin-Jiang He: Formal analysis, investigation, validation, writing–original draft preparation; Sha Lin: Conceptualization, methodology, software, writing–reviewing and editing. All authors have read and agreed to the published version of the manuscript.

Use of Generative-AI tools declaration

The authors declare that they have not used Artificial Intelligence (AI) tools in the creation of this article.

Acknowledgments

This work is supported by the National Natural Science Foundation of China (No. 12301614, No. 12101554), Zhejiang Provincial Philosophy and Social Sciences Planning Project (No. 26NDJC019YB), Fundamental Research Funds for Zhejiang Provincial Universities (No. GB202103001), and Research Project of Zhejiang Federation of Humanities and Social Sciences (No. 2025N095). The authors would also like to gratefully acknowledge the anonymous referees' constructive comments and suggestions, which greatly helped to improve the quality and readability of the manuscript.

Conflict of interest

The authors have no relevant financial or non-financial interests to disclose.

References

1. M. Abudy, Y. Izhakian, Pricing stock options with stochastic interest rate, *Int. J. Portfolio Anal. Manage.*, **1** (2013), 250–277. https://doi.org/10.1504/IJPAM.2013.054408

2. R. Ahlip, M. Rutkowski, Pricing of foreign exchange options under the Heston stochastic volatility model and CIR interest rates, *Quant. Financ.*, **13** (2013), 955–966. https://doi.org/10.1080/14697688.2013.769688

3. G. Bakshi, C. Cao, Z. Chen, Empirical performance of alternative option pricing models, *J. Financ.*, **52** (1997), 2003–2049. https://doi.org/10.1111/j.1540-6261.1997.tb02749.x

4. S. Beckers, Variances of security price returns based on high, low, and closing prices, *J. Bus.*, **56** (1983), 97–112.

5. F. Black, M. Scholes, The pricing of options and corporate liabilities, *J. Polit. Econ.*, **81** (1973), 637–654.

6. B. S. K. Bolaky, J. Narsoo, N. Thakoor, D. Y. Tangman, M. Bhuruth, Deep neural networks for the valuation of equity and real-estate index American options under models with stochastic volatility, *China Financ. Rev. Int.*, 2025, 1–27. https://doi.org/10.1108/CFRI-07-2024-0389

7. D. Brigo, F. Mercurio, *Interest rate models-theory and practice: With smile, inflation and credit*, Springer Science & Business Media, 2006.

8. J. Buffington, R. J. Elliott, American options with regime switching, *Int. J. Theor. Appl. Fin.*, **5** (2002), 497–514. https://doi.org/10.1142/S0219024902001523

9. J. Cao, T. R. N. Roslan, W. Zhang, Pricing variance swaps in a hybrid model of stochastic volatility and interest rate with regime-switching, *Methodol. Comput. Appl.*, **20** (2018), 1359–1379. https://doi.org/10.1007/s11009-018-9624-5

10. J. Cao, T. R. N. Roslan, W. Zhang, The valuation of variance swaps under stochastic volatility, stochastic interest rate and full correlation structure, *J. Korean Math. Soc.*, **57** (2020), 1167–1186. https://doi.org/10.4134/JKMS.j190616

11. W. Chen, X. J. He, An analytical approximation for European options under a Heston-type model with regime switching, *N. Am. J. Econ. Financ.*, **80** (2025), 102500. https://doi.org/10.1016/j.najef.2025.102500

12. W. Chen, Z. Yang, X. J. He, Pricing energy futures options: The role of seasonality and liquidity, *Energ. Econ.*, **149** (2025), 108737. https://doi.org/10.1016/j.eneco.2025.108737

13. P. Christoffersen, S. Heston, K. Jacobs, The shape and term structure of the index option smirk: Why multifactor stochastic volatility models work so well, *Manage. Sci.*, **55** (2009), 1914–1932. https://doi.org/10.1287/mnsc.1090.1065

14. P. Christoffersen, K. Jacobs, The importance of the loss function in option valuation, *J. Financ. Econ.*, **72** (2004), 291–318. https://doi.org/10.1016/j.jfineco.2003.02.001

15. P. Christoffersen, K. Jacobs, K. Mimouni, An empirical comparison of affine and non-affine models for equity index options, *SSRN Electron. J.*, 2006.

16. B. Dumas, J. Fleming, R. E. Whaley, Implied volatility functions: Empirical tests, *J. Financ.*, **53** (1998), 2059–2106. https://doi.org/10.1111/0022-1082.00083

17. R. J. Elliott, L. Aggoun, J. B. Moore, *Hidden Markov models: Estimation and control*, Springer Science & Business Media, **29** (2008).

18. R. J. Elliott, G. H. Lian, Pricing variance and volatility swaps in a stochastic volatility model with regime switching: Discrete observations case, *Quant. Financ.*, **13** (2013), 687–698. https://doi.org/10.1080/14697688.2012.676208

19. F. Fang, C. W. Oosterlee, A Fourier-based valuation method for Bermudan and barrier options under heston's model, *SIAM J. Financ. Math.*, **2** (2011), 439–463. https://doi.org/10.1137/100794158

20. J. Gatheral, T. Jaisson, M. Rosenbaum, Volatility is rough, *Quant. Financ.*, **18** (2018), 933–949. https://doi.org/10.1080/14697688.2017.1393551

21. C. A. Grajales, S. Medina Hurtado, S. Mongrut, Pricing, risk and hedging of European options: uncertainty versus stochastic approaches, *China Financ. Rev. Int.*, **15** (2025), 821–843. https://doi.org/10.1108/CFRI-10-2024-0606

22. L. A. Grzelak, C. W. Oosterlee, On the Heston model with stochastic interest rates, *SIAM J. Financ. Math.*, **2** (2011), 255–286. https://doi.org/10.1137/090756119

23. L. A. Grzelak, C. W. Oosterlee, S. V. Weeren, Extension of stochastic volatility equity models with the Hull–White interest rate process, *Quant. Financ.*, **12** (2012), 89–105. https://doi.org/10.1080/14697680903170809

24. J. D. Hamilton, Analysis of time series subject to changes in regime, *J. Econometrics*, **45** (1990), 39–70. https://doi.org/10.1016/0304-4076(90)90093-9

25. X. J. He, H. Chen, S. Lin, A closed-form formula for pricing European options with stochastic volatility, regime switching, and stochastic market liquidity, *J. Futures Markets*, **45** (2025), 429–440. https://doi.org/10.1002/fut.22573

26. X. J. He, W. Chen, T. Lu, S. Lin, Variance and volatility swap valuation with stochastic liquidity and regime switching stochastic volatility, *Commun. Nonlinear Sci.*, **154** (2026), 109558. https://doi.org/10.1016/j.cnsns.2025.109558

27. X. J. He, S. Lin, Analytically pricing foreign exchange options under a three-factor stochastic volatility and interest rate model: A full correlation structure, *Expert Syst. Appl.*, **246** (2024), 123203. https://doi.org/10.1016/j.eswa.2024.123203

28. X. J. He, W. Wei, S. Lin, A closed-form formula for pricing exchange options with regime switching stochastic volatility and stochastic liquidity, *Int. Rev. Financ. Anal.*, **103** (2025), 104159. https://doi.org/10.1016/j.irfa.2025.104159

29. S. L. Heston, A closed-form solution for options with stochastic volatility with applications to bond and currency options, *Rev. Financ. Stud.*, **6** (1993), 327–343. https://doi.org/10.1093/rfs/6.2.327

30. S. Y. Hong, H. M. Zhang, Y. Q. Lu, Y. Y. Jiang, A closed-form pricing formula for European options under a multi-factor nonlinear stochastic volatility model with regime-switching, *Jpn J. Ind. Appl. Math.*, **41** (2024), 1079–1095. https://doi.org/10.1007/s13160-023-00642-2

31. J. Hull, A. White, The pricing of options on assets with stochastic volatilities, *J. Financ.*, **42** (1987), 281–300. https://doi.org/10.1111/j.1540-6261.1987.tb02568.x

32. L. Ingber, Very fast simulated re-annealing, *Math. Comput. Model.*, **12** (1989), 967–973. https://doi.org/10.1016/0895-7177(89)90202-1

33. L. Ingber, Home page of Lester Ingber, 2025.

34. H. A. O. Junior, L. Ingber, A. Petraglia, M. R. Petraglia, M. A. S. Machado, *Adaptive simulated annealing*, In: Stochastic global optimization and its applications with fuzzy adaptive simulated annealing, Springer, **35** (2012), 33–62. https://doi.org/10.1007/978-3-642-27479-4_4

35. H. Johnson, D. Shanno, Option pricing when the variance is changing, *J. Financ. Quant. Anal.*, **22** (1987), 143–151. https://doi.org/10.2307/2330709

36. S. Kirkpatrick, C. D. Gelatt, M. P. Vecchi, Optimization by simmulated annealing, *Science*, **220** (1983), 671–680. https://doi.org/10.1126/science.220.4598.671

37. A. Le, Separating the components of default risk: A derivative-based approach, *Q. J. Financ.*, **5** (2015), 1550005. https://doi.org/10.1142/S2010139215500056

38. S. Lin, M. Chen, X. J. He, Analytically pricing crude oil options under a jump-diffusion model with stochastic liquidity risk and convenience yield, *N. Am. J. Econ. Financ.*, **78** (2025), 102424. https://doi.org/10.1016/j.najef.2025.102424

39. S. Lin, X. J. He, Analytically pricing variance and volatility swaps with stochastic volatility, stochastic equilibrium level and regime switching, *Expert Syst. Appl.*, **217** (2023), 119592. https://doi.org/10.1016/j.eswa.2023.119592

40. C. Ma, S. Yue, H. Wu, Y. Ma, Pricing vulnerable options with stochastic volatility and stochastic interest rate, *Comput. Econ.*, **56** (2020), 391–429. https://doi.org/10.1007/s10614-019-09929-4

41. F. Mehrdoust, N. Saber, Pricing arithmetic Asian option under a two-factor stochastic volatility model with jumps, *J. Stat. Comput. Sim.*, **85** (2015), 3811–3819. https://doi.org/10.1080/00949655.2015.1046072

42. S. Mikhailov, U. Nögel, *Heston's stochastic volatility model: Implementation, calibration and some extensions*, John Wiley and Sons, 2004.

43. P. Pasricha, X. J. He, Vulnerable options under a Hawkes jump-diffusion model with two-factor stochastic volatility, *Int. Rev. Financ. Anal.*, **111** (2026), 105095. https://doi.org/10.1016/j.irfa.2026.105095

44. W. P. Koziell, *Stochastic volatility models: Calibration, pricing and hedging*, PhD thesis, University of the Witwatersrand, Johannesburg, 2012.

45. R. Schöbel, J. Zhu, Stochastic volatility with an Ornstein–Uhlenbeck process: An extension, *Eur. Financ. Rev.*, **3** (1999), 23–46. https://doi.org/10.1023/A:1009803506170

46. L. O. Scott, Option pricing when the variance changes randomly: Theory, estimation, and an application, *J. Financ. Quant. Anal.*, **22** (1987), 419–438. https://doi.org/10.2307/2330793

47. J. Shu, J. E. Zhang, Pricing S&P 500 index options under stochastic volatility with the indirect inference method, *J. Deriv. Account.*, **1** (2004), 1–16. https://doi.org/10.1142/S021986810400021X

48. T. K. Siu, H. Yang, J. W. Lau, Pricing currency options under two-factor Markov-modulated stochastic volatility models, *Insur. Math. Econ.*, **43** (2008), 295–302. https://doi.org/10.1016/j.insmatheco.2008.05.002

49. E. M. Stein, J. C. Stein, Stock price distributions with stochastic volatility: An analytic approach, *Rev. Financ. Stud.*, **4** (1991), 727–752. https://doi.org/10.1093/rfs/4.4.727

50. M. T. Vo, Regime-switching stochastic volatility: Evidence from the crude oil market, *Energ. Econ.*, **31** (2009), 779–788. https://doi.org/10.1007/s10529-009-9933-4

51. X. Wang, W. Xiao, J. Yu, Modeling and forecasting realized volatility with the fractional Ornstein–Uhlenbeck process, *J. Econometrics*, **232** (2023), 389–415. https://doi.org/10.1016/j.jeconom.2021.08.001

52. J. B. Wiggins, Option values under stochastic volatility: Theory and empirical estimates, *J. Financ. Econ.*, **19** (1987), 351–372. https://doi.org/10.1016/0304-405X(87)90009-2

53. H. Wu, Z. Jia, S. Yang, C. Liu, Pricing variance swaps under double heston stochastic volatility model with stochastic interest rate, *Probab. Eng. Inform. Sci.*, **36** (2022), 564–580. https://doi.org/10.1017/S0269964820000662

54. D. Yan, X. J. Huang, G. Ma, X. J. He, Pricing American options with exogenous and endogenous transaction costs, *Comput. Math. Appl.*, **200** (2025), 85–101. https://doi.org/10.1016/j.camwa.2025.09.008

55. D. Yan, W. Ye, X. J. He, American option pricing under a two-factor stochastic volatility model with nonlinear exogenous costs, *Math. Method. Appl. Sci.*, **48** (2025), 14868–14879. https://doi.org/10.1002/mma.11219

56. B. Z. Yang, J. Yue, N. J. Huang, Equilibrium price of variance swaps under stochastic volatility with Lévy jumps and stochastic interest rate, *Int. J. Theor. Appl. Financ.*, **22** (2019), 1950016. https://doi.org/10.1142/S021902491950016X

57. Y. Yang, S. Liu, Y. Wu, B. Wiwatanapataphee, Pricing of volatility derivatives in a Heston–CIR model with Markov-modulated jump diffusion, *J. Comput. Appl. Math.*, **393** (2021), 113277. https://doi.org/10.1016/j.cam.2020.113277

58. T. Zaevski, On the ϵ-optimality of American options, *China Financ. Rev. Int.*, **15** (2025), 688–714. https://doi.org/10.1108/CFRI-06-2024-0361

AIMS Press